Open Access Journal

**Journal of Power Technologies 97 (1) (2017) 35–43**

journal homepage:papers.itc.pw.edu.pl

# Banes and Boons of Perturb & Observe, Incremental Conductance and Modified Regula Falsi Methods for Sustainable PV Energy Generation

Yatindra Gopal*, Krishn Kumar, Dinesh Birla, Mahendra Lalwani

*Department of Electrical Engineering, Rajasthan Technical University, Kota, Rajasthan, India-324010*

**Abstract**

Maximum power point tracking (MPPT) optimizes overall power generation in photovoltaic (PV) applications. The voltage-power characteristics of PV array operating under variable irradiance and temperature conditions exhibit numerous local maximum power points (MPP). This paper presents the optimization method of MPP tracking, based on the modified Regula Falsi method (MRFM). Results of this method are compared with the conventional perturb & observe (P&O) method and the incremental conductance (IC) method. The modified Regula Falsi method has better convergence, lower oscillation time, less power loss and enhanced output power than the other two methods. To obtain a stable voltage from a solar array, a DC-DC Cuk converter is used. It can step-up and step-down the voltage level according to load requirement. Results have been verified on the MATLAB platform in variable environmental conditions.

*Keywords:* Photovoltaic, Maximum power point tracking, Perturb & observe, Incremental conductance, Modified Regula Falsi method, Cuk converter.

## 1. Introduction

In the last few decades, there has been dramatic increase in the demand for electricity. This looks set to continue indefinitely due to general socio-economic development [22, 17]. Recently, PV has emerged as an alternative energy source, supporting the existing conventional power generation system. However, PV has the following major challenges:

1. Optimal utilization of the source due to its nonlinear characteristics [e.g., MPPT is needed to track maximum power from PV array].
2. It is usually operated at a low voltage output level (25-50V). Therefore, a DC-DC Cuk converter is used to step-up and step-down the voltage level as per load requirement [10].

Points 1. and 2. above necessitate the use of MPPT & a DC-DC Cuk converter [10, 8]. In recent years different MPPT techniques have been developed [8, 12]. These MPPT techniques can be divided into two groups. The first group is based on voltage feedback. Here, the reference voltage is compared with PV module voltage in a feedback loop. The drawback of this method is loss of energy during momentary interruptions. In the second group of techniques, the feedback power method based on calculation is used [12]. In the feedback power method, the algorithms majority attempt to keep the ratio dP/dV at zero. Among the reported methods, the P&O technique is popular and simple to execute [22, 8, 14]. This method involves more energy loss and fixed step size to consider interface with a DC-DC converter; so that the operating point does not deviate away from MPP, as the environmental state changes frequently [22, 8, 12, 5, 20]. The IC method also keeps the ratio dP/dV at zero. Thus in the IC method, the slope of the PV array power curve is zero at MPP (Pmax). In this method, MPP can be found by comparing incremental conductance to instantaneous conductance. It stops the oscillation problem around MPP at fixed step size [22, 12, 19, 4, 11]. Due to fixed step size and low convergence, both the P&O and IC methods are considered as a trial and inaccuracy course [19, 20, 4]. This paper presents a comprehensive comparison of P&O, IC and MRFM based on output energy, convergence speed, duty cycle, oscillation near MPP, power loss etc. The MRFM is well suitable for MPPT because root convergence can be achieved without observing oscillation near MPP [23]. This method provides fast convergence and inconsistent step size; thereby improving energy extraction from the PV array and enhancing performance under changing environmental conditions [8, 14, 23].

*Corresponding author
*Email address:* hellogopal4u@gmail.com (Yatindra Gopal)

## 2. Mathematical Modeling of PV Module

The current-voltage relationship of this mathematical model is specified by the following equation [16].

$$I = I_{sc} - I_0\left[e^{q\left(\frac{V+I\cdot R_S}{nKT}\right)} - 1\right] \tag{1}$$

where: $V$—cell voltage, $I$—cell current, $R_S$—PV cell series resistance, $I_0$—reverse saturation current, $n$—ideality factor, $I_{sc}$—short–cicrcuit current, $T$—cell temperature.

At any temperature of cell $T$, Short-circuit current $I_{sc}$ is given as under:

$$I_{sc}|_T = I_{sc}|T_{ref} \cdot \left[1 + a\left(T - T_{ref}\right)\right] \tag{2}$$

where: $T_{ref}$—reference temperature of PV cell in Kelvin measured at irradiance of 1,000 W/m$^2$ and $\alpha$ is the temperature coefficient of $I_{cs}$.

The short - circuit current $I_{sc}$ is proportional to the intensity of irradiance. $I_{sc}$ at a specified irradiance $G$ is given by the equation below:

$$I_{sc}|_G = \left\{\frac{G}{G_0}\right\} I_{sc}|_{G_0} \tag{3}$$

where: $G_0$is the nominal value of irradiance in $W/m^2$. The reverse saturation current $I_0$ is temperature dependant and can be considered by the following equation.

$$I_0|_T = I_0|_{T_{ref}} \cdot \left\{\frac{T}{T_{ref}}\right\}^{\frac{n}{3}} \cdot e^{\frac{-qE_g}{nK}\left\{\frac{1}{T} - \frac{1}{T_{ref}}\right\}} \tag{4}$$

where: $n$—diode ideality factor is equalt to 1.62, $E_g$—the band gap voltage for silicon is 1.1eV.

The output current (I) is computed by Newton's method iteratively.

$$I_{n+1} = I_n - \frac{I_{sc} - I_n - I_0\left[e^{q\left(\frac{V+I_n\cdot R_s}{nKT}\right)} - 1\right]}{-1 - I_0\left(\frac{q\cdot R_S}{nKT}\right)e^{q\left(\frac{V+I_n\cdot R_S}{nKT}\right)}} \tag{5}$$

This iterative process can be concluded when the difference between $1_{n+1}$ and $n$ reaches an acceptably small value. The MATLAB function written in this paper performs the calculation five times iteratively to ensure convergence. The testing result showed that the value of In usually converges within three iterations and never more than four interactions.

## 3. DC-DC Converter (Cuk Converter)

Switch mode power supply DC-DC converters, based on MOSFETS, IGBTS are used for many industrial applications at present. A converter is installed mainly to produce constant voltage, capacitive isolation to protect against switch failure and deliver maximum power from the solar array to load [10, 5, 9, 13, 11]. In this work the DC-DC Cuk converter used is based on the MOSFET switch shown in Fig. 1.

In steady state, the average inductor voltage is zero. The primary state of switch (SW) is off and input voltage is applied. Diode (D1) is forward biased and the capacitor (C1) is charged. The operation mode of the circuit is divided into two modes:

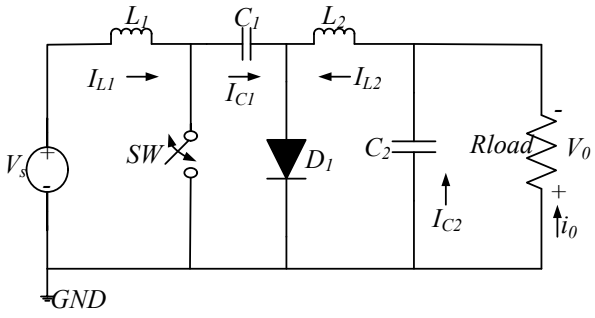


Figure 1: Basic circuit diagram of Cuk converter

Table 1: Design Specification of the Cuk converter

| Different Electrical Parameter Requirement | |
|---|---|
| Input Voltage ($V_S$) | 20–48 V |
| Input Current ($I_S$) | 0–5 A (< 5% ripple) |
| Output Voltage ($V_0$) | 12–30 V (< 5% ripple) |
| Output Current ($I_0$) | 0–5 A (< 5% ripple) |
| Duty Cycle ($D$) | 0.1 < D < 0.6 |
| Switching Frequency ($f$) | 50 kHz |
| Maximum Output Power ($P_{max}$) | 150 W |

1. When MOSFET is turned on at $t = 0$, current through inductor ($L_1$) rises, at the same time voltage of ($C_1$) reverse biases diode ($D_1$) and turns it off. ($C_1$) discharges energy to the circuit $C_1$-$C_2$-Rload-inductor ($L_2$).
2. When MOSFET switch is turned off at $t = t_1$, the capacitor will charge from input supply ($V_S$) and will transfer stored energy of the inductor to the load. Thus energy is transferred from source to Rload through the capacitor ($C_1$) [5].

- when, switch (SW) turns ON, $-I_{C1} = I_{L2}$
- when, swtich turns OFF, $I_{C1} = I_{L1}$

$$\frac{I_{L1}}{I_{L2}} = \frac{D}{1-D} \tag{6}$$

$$\frac{V_0}{V_s} = \frac{D}{1-D} \tag{7}$$

The Cuk converter is designed based on the requirements shown below in Table 1.

The values of $L_1$, $L_2$, $C_1$ and $C_2$ used in converter are as follows: $L_1 = 1.475\,mH$, $L_2 = 1.283\,mH$, $C_1 = 14.42\,\mu F$ $C_2 = 0.3567\,\mu F$. Diode $D_1$ is chosen due to its good reverse recovery time (usually 5 to 10 ns), low forward voltage and Power–MOSFET switches are chosen for low to medium power applications.

## 4. Perturb & observe algorithm

The (P&O) algorithm is very common and the one most suitable for practical application. The operating voltage of the

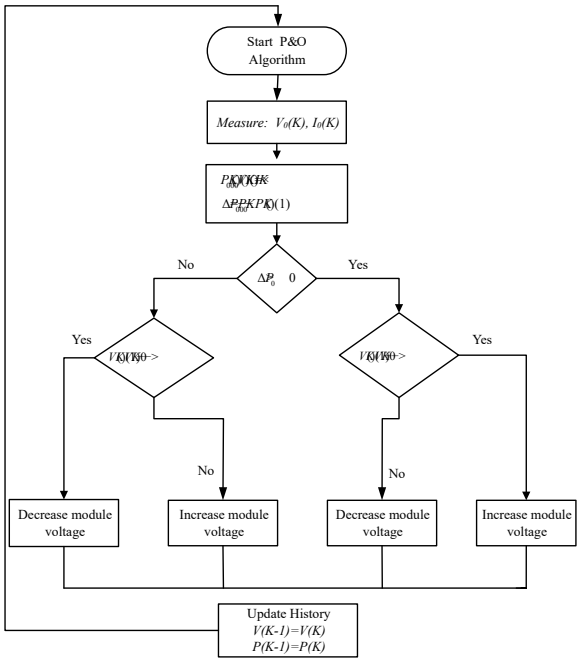


Figure 2: P&O algorithm flowchart

PV module is perturbed by a small increment and the resulting change in power ($\Delta P$) is observed. If the $\Delta P$ is positive, then it is considered that the operating point has achieved near to MPP. If the $\Delta P$ is negative, the operating point has moved away from MPP and the perturbation direction is reversed to move back toward MPP [6, 15, 2]. A flowchart of the P&O algorithm is given in Fig. 2.

## 5. Incremental conductance (IC) algorithm

The basic idea of the algorithm is that P-V curve slope becomes zero at MPP. The derivative of slope of PV module's power with respect to PV voltage has the following relations with MPP [22, 8, 20, 16, 2, 18].

$$\frac{\Delta P}{\Delta V} = 0 \; at \; MPP, \; \frac{\Delta P}{\Delta V} > 0 \; at \; the \; left \; of \; MPP, \\ \frac{\Delta P}{\Delta V} < 0 \; at \; the \; right \; of \; MPP \tag{8}$$

If the operating point is at MPP:

$$\frac{dI}{dV} = -\frac{I}{V} \tag{9}$$

If the operating point is to the left of MPP:

$$\frac{dI}{dV} > -\frac{I}{V} \tag{10}$$

If the operating point is to the right of MPP:

$$\frac{dI}{dV} < -\frac{I}{V} \tag{11}$$

where: $dI/dV$ is an incremental conductance and $I/V$ is instantaneous conductance.

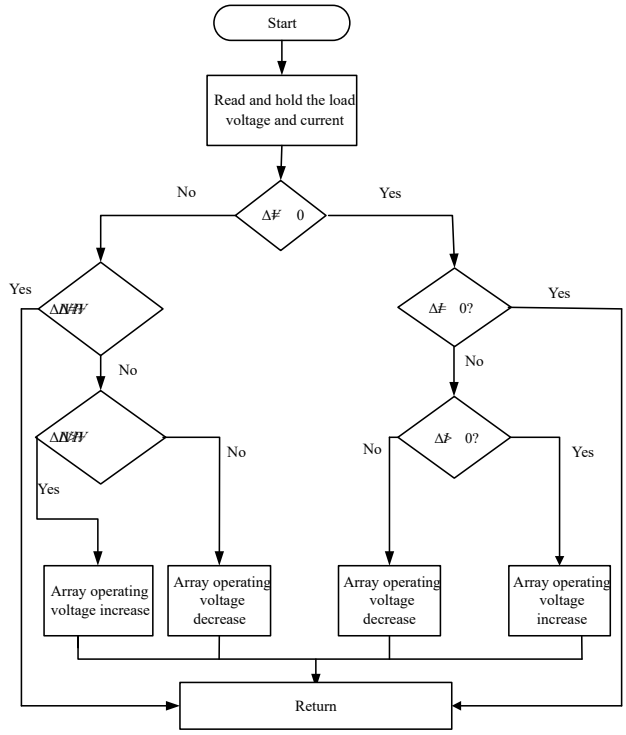


Figure 3: Flowchart of the IC algorithm

From equation 9 MPP can be found by comparing instantaneous conductance to the incremental conductance [20, 4, 7, 21]. The flowchart of the IC algorithm is shown in Fig. 3.

## 6. Modified Regula Falsi method (MRFM) algorithm

The RFM (Regula Falsi method) convergent is a linearly root-finding algorithm as function is continuous with one independent variable shown in Fig. 4 [23]. This algorithm finds first initial bracketing point $x_1$ and $x_u$ for continuous function $f(x)$. Calculating from the equation 12 approximate value for the root $c_i$ at every iteration $i$.

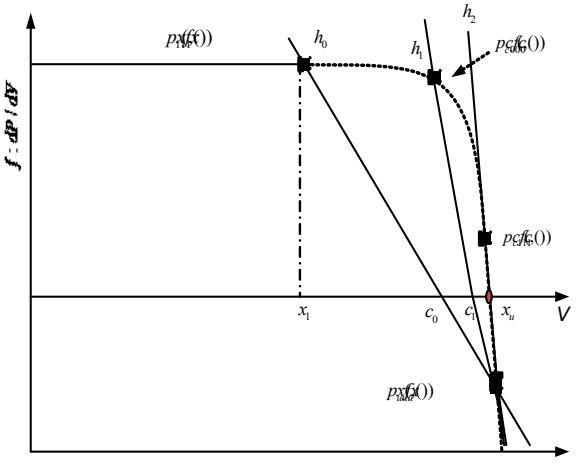


Figure 4: Regula Falsi method (RFM)

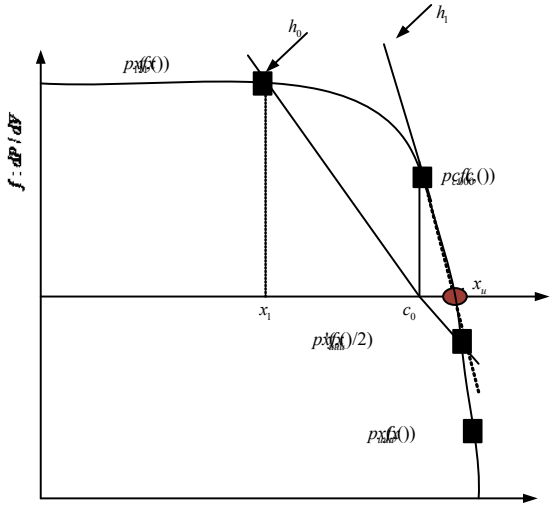


Figure 5: Modified Regula falsi method

$$c_i = \frac{x_1 \cdot f(x_u) - x_u \cdot f(x_1)}{f(x_u) - f(x_1)} \tag{12}$$

where: $i = 0, 1, 2, 3, ...$

When $f(c_i) = 0$ then ci is root otherwise $f(c_i)$. $f(x_u) < 0$ then consider $x_1 = c_i$, or if $f(c_i)$. $f(x_1) < 0$ then consider $x_u = c_i$. The result of this RFM procedure smaller size bracketing interval because bracketed interval is constant of one end point. This problem is improved by the MRFM as shown in Fig. 5 which is similar to the RFM. While calculate the next root iteration approximation, $c_i$, the following processes is taken instead of the abovementioned step of the RFM in 12.

If, $f(x_1) \cdot f(x_u) < 0$ and $f(x_1) > 0$ then, $f(x_u)$ is replaced in equation 12 by $f_p(x_u) = \frac{f(x_u)}{2}$ and $f_p(x_1) = f(x_1)$

$$c_i = \frac{x_1 \cdot f_p(x_u) - x_u \cdot f_p(x_1)}{f_p(x_u) - f_p(x_1)} = \\ = \frac{x_1 \cdot f(x_u) \cdot 0.5 - x_u \cdot f(x_1)}{0.5 \cdot f(x_u) - f(x_1)} \tag{13}$$

where: $i = 1, 2, 3, ...$

If, $f(x_1) \cdot f(x_u) < 0$ and $f(x_1) < 0$ then, $f(x_1)$ is replaced in equation 12 by $f_p(x_1) = \frac{f(x_1)}{2}$ and $f_p(x_u) = f(x_u)$

$$c_i = \frac{x_1 \cdot f_p(x_u) - x_u \cdot f_p(x_1)}{f_p(x_u) - f_p(x_1)} = \\ = \frac{x_1 \cdot f(x_u) - x_u \cdot f(x_1) \cdot 0.5}{f(x_u) - 0.5 \cdot f(x_1)} \tag{14}$$

where: $i = 1, 2, 3, ...$

These changes effectively decrease the magnitude of by $1/2$ at one of the brackets ends in order to achieve faster convergence [8, 23]. MRFM flow chart is shown in Fig. 6. The algorithm consists of three major modes, which are the initial mode, the MPPT mode and the Idle mode. After the sampling process in the initial MPPT mode $\Delta V$ is known. Hence this information can be used to detect if an irradiation change has occurred.

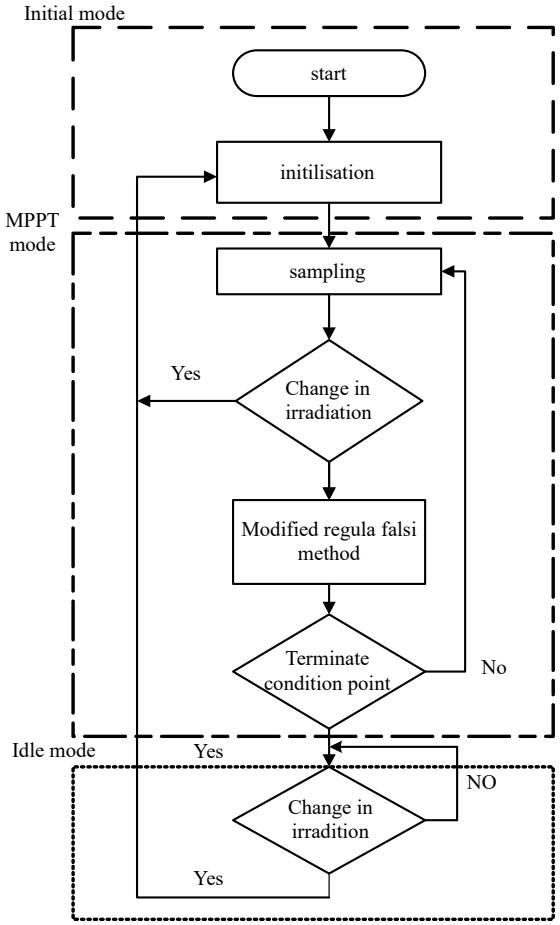


Figure 6: MRFM Flow Chart

## 7. Results and comparision

In order to perform comparative analysis of considered MPPT techniques, BP SX 150B solar PV module has been used in MATLAB platform. The module consists of 72 multicrystalline silicon solar cells are connected in series, an ideal Cuk converter, 6Ω resistive load and 150W of nominal maximum power. The technical parameter values of solar PV panel are shown in Table 2. For a Cuk converter the input and output of voltage and current relationship equations are given by equation 15. These equations are used in the MATLAB programming.

$$V_0 = \frac{D}{1-D} \cdot V_s \quad I_0 = \frac{1-D}{D} \cdot I_s \tag{15}$$

where: $V_0$, $I_0$—Cuk converter output voltage and current, $V_s$, $I_s$—input voltage and current, $D$—duty cycle of the Cuk converter.

The programming is performed under the linearly increasing irradiance. Fig. 7 shows the graphs between output powers (W) tracked by the three MPPT techniques (P&O, IC, and MRFM) and modular voltage (V). From graphs, it is observed that the P&O, IC techniques are slower in tracking MPP compared to the MRFM technique.

Table 2: Technical parameter values of PV module of BP SX 150B solar PV panel [1]

| Electrical parameters | Icon | Specification |
|---|---|---|
| Maximum power (Watt) | $P_{max}$ | 150 |
| Maximum power voltage (V) | $V_{mpp}$ | 34.5 |
| Maximum power current (A) | $I_{mpp}$ | 4.35 |
| Open–circuit voltage (V) | $V_{oc}$ | 43.5 |
| Short–circuit current (A) | $I_{SC}$ | 4.75 |
| Temperature coefficient of $I_{SC}$(V/℃) | $K_v$ | 0.065±0.015% |
| Temperature coefficient of $V_{oc}$ (mV/℃) | $K_i$ | -160±20 |
| Temperature coefficient of power | $K_p$ | -0.5±0.05% |
| Nominal operating cell temperature NOCT (℃) | - | 47±2 |

Fig. 8 shows the graph modular current (A) and modular voltage (V), it indicates that P&O, IC technique convergence speed is less. The MRFM technique has faster convergence speed, guarantees reaching MPP, and has less power loss than the P&O and IC techniques.

Fig. 9 shows the graph between converter output powers (W) tracked by the three MPPT techniques (P&O, IC and MRFM) and duty cycle. It indicates that the duty cycle varies less with the P&O and IC techniques than in the MRFM technique.

The comparison of the graph between the converter output powers (W) tracked by the three MPPT techniques and duty cycle is shown in Fig. 10. From the graphs, it is observed that in the P&O technique the duty cycle during the whole operation varies from 0.2 to 0.5, the IC technique duty cycle varies from 0.15 to 0.45; both have fixed size in step. However, the MRFM duty cycle varies from 0.1 to 0.5 which is variable step size having less oscillation in the duty cycle.

The graph between the converter output current (A) tracked by the three MPPT techniques (P&O, IC and MRFM) and the output voltage is shown in Fig. 11. From the graphs, it is observed that the P&O, IC techniques during the whole process have more variations or changes in Cuk converter output current with voltage than does the MRFM technique.

The P&O, IC and MRFM techniques are programmed and compared under the same conditions. When atmospheric conditions change slowly or are constant, the P&O and IC MPPT oscillations are quite close to MPP, but MRFM finds MPP accurately in changing atmospheric conditions. Table 3 shows a comparison of the three techniques for different properties. The MRFM is observed to be the fastest among the three techniques to find convergence to MPP. It reaches MPP immediately, in contrast to fixed step size algorithms (e.g., P&O and IC), and the MRFM step size varies while approaching MPP; hence the MRFM technique is more accurate.

## 8. Conclusion

Photovoltaic systems are one of the vital technologies envisioned to achieve suitable energy generation. The system is interfaced with various essential power electronics components to achieve the necessary efficiency in energy conversion to harness renewable energy. In this paper, a comparative MPPT analysis is made of the P&O, IC and MRFM methods. MPPT methods are key enablers of a more energy sustainable society, due to their ease of use, low cost and malleable operation. The analysis was validated on a MATLAB platform in variable irradiance and temperature conditions. It is observed that MRFM enjoys better performance than the P&O and IC techniques. These three techniques improve the steady state and dynamics performance for photovoltaic systems and improve the performance of the DC-DC converter. Based on the analysis it is observed that the variable step MRFM method is the fastest technique of the three compared techniques to reach MPP in a total of four iterations.

## References


[1] BP Solar BP SX 150-150B Multi-crystalline Photovoltaic Module Datasheet, 2003.

[2] Bader N Alajmi, Khaled H Ahmed, Stephen J Finney, and Barry W Williams. Fuzzy-logic-control approach of a modified hill-climbing method for maximum power point in microgrid standalone photovoltaic system. *IEEE Transactions on Power Electronics*, 26(4):1022–1030, 2011.

[3] Saleh Elkelani Babaa, Matthew Armstrong, and Volker Pickert. Overview of maximum power point tracking control methods for pv systems. *Journal of Power and Energy Engineering*, 2014(2 (8)):59–72, 2014.

[4] Ioan Viorel Banu, Răzvan Beniugă, and Marcel Istrate. Comparative analysis of the perturb-and-observe and incremental conductance mppt methods. In *Advanced Topics in Electrical Engineering (ATEE), 2013 8th International Symposium on*, pages 1–4. IEEE, 2013.

[5] Srushti R Chafle, Uttam B Vaidya, and ZJ Khan. Design of cuk converter with mppt technique. *International journal of innovative research in electrical, electronics, instrumentation and control engineering*, 1(4): 161–167, 2013.

[6] I William Christopher and R Ramesh. Comparative study of p&o and inc mppt algorithms. *American Journal of Engineering Research*, 2 (12):402–408, 2013.

[7] Seunghyun Chun and Alexis Kwasinski. Analysis of classical root-finding methods applied to digital maximum power point tracking for sustainable photovoltaic energy generation. *IEEE Transactions on Power Electronics*, 26(12):3730–3743, 2011.

[8] Seunghyun Chun and Alexis Kwasinski. Modified regula falsi optimization method approach to digital maximum power point tracking for photovoltaic application. In *Applied Power Electronics Conference and Exposition (APEC), 2011 Twenty-Sixth Annual IEEE*, pages 280–286. IEEE, 2011.

[9] Moumita Das and Vivek Agarwal. Novel high-performance stand-alone solar pv system with high-gain high-efficiency dc–dc converter power stages. *IEEE Transactions on Industry Applications*, 51(6):4718–4728, 2015.

[10] Moumita Das and Vivek Agarwal. Design and analysis of a high-efficiency dc–dc converter with soft switching capability for renewable energy applications requiring high voltage gain. *IEEE Transactions on Industrial Electronics*, 63(5):2936–2944, 2016.

[11] Trishan Esram and Patrick L Chapman. Comparison of photovoltaic array maximum power point tracking techniques. *IEEE Transactions on energy conversion*, 22(2):439–449, 2007.

[12] Nicola Femia, Giovanni Petrone, Giovanni Spagnuolo, and Massimo Vitelli. A technique for improving p&o mppt performances of double-stage grid-connected photovoltaic systems. *IEEE Transactions on Industrial Electronics*, 56(11):4473–4482, 2009.

[13] N Fermia, D Granozio, G Petrone, and M Vitelli. Predictive & adaptive mppt perturb and observe method. *IEEE Transactions on Aerospace and Electronic Systems*, 43(3):934–950, 2007.

[14] Joonhyun Kim and Alexis Kwasinski. Maximum power point tracking for multiple photovoltaic modules using root-finding methods. In *Energy Conversion Congress and Exposition (ECCE), 2014 IEEE*, pages 9–16. IEEE, 2014.

Table 3: Comparison of P&O, IC and MRFM MPPT techniques

| S. No. | Property | P&O | IC | MRFM |
|---|---|---|---|---|
| 1 | Output energy | 75.3159 kWh | 75.2636 kWh | 75.4241 |
| 2 | Convergence speed | Medium | High | Fast |
| 3 | Oscilation near MPP | Medium | High | Less |
| 4 | Converter duty cycle | Fixed step size | Fixed step size | Variable step |
| 5 | Impementation complexity | Easy | Complex | Medium |
| 6 | Power loss | More | Depends on duty cycle | Less |
| 7 | Control variable | V and I | V and I | V, I and D |

[15] Tey Kok Soon, Saad Mekhilef, and Azadeh Safari. Simple and low cost incremental conductance maximum power point tracking using buck-boost converter. *Journal of Renewable and Sustainable Energy*, 5(2): 023106, 2013.

[16] Rajan Kumar and Bhim Singh. Solar pv array fed cuk converter-vsi controlled bldc motor drive for water pumping. In *Power India International Conference (PIICON), 2014 6th IEEE*, pages 1–7. IEEE, 2014.

[17] Mahendra Lalwani, DP Kothari, and Mool Singh. Size optimization of stand-alone photovoltaic system under local weather conditions in india. *International Journal of Applied Engineering Research*, 1(4): 951–962, 2011.

[18] Rasoul Rahmani, Mohammadmehdi Seyedmahmoudian, Saad Mekhilef, and Rubiyah Yusof. Implementation of fuzzy logic maximum power point tracking controller for photovoltaic system. *American Journal of Applied Sciences*, 10(3):209–218, 2013.

[19] Azadeh Safari and Saad Mekhilef. Simulation and hardware implementation of incremental conductance mppt with direct control method using cuk converter. *IEEE transactions on industrial electronics*, 58(4): 1154–1161, 2011.

[20] Dezso Sera, Laszlo Mathe, Tamas Kerekes, Sergiu Viorel Spataru, and Remus Teodorescu. On the perturb-and-observe and incremental conductance mppt methods for pv systems. *IEEE journal of photovoltaics*, 3(3):1070–1078, 2013.

[21] Yong Tian, Bizhong Xia, Zhihui Xu, and Wei Sun. Modified asymmetrical variable step size incremental conductance maximum power point tracking method for photovoltaic systems. *Journal of Power Electronics*, 14(1):156–164, 2014.

[22] Deepak Verma, Savita Nema, AM Shandilya, and Soubhagya K Dash. Maximum power point tracking (mppt) techniques: Recapitulation in solar photovoltaic systems. *Renewable and Sustainable Energy Reviews*, 54:1018–1034, 2016.

[23] Weidong Xiao, Ammar Elnosh, Vinod Khadkikar, and Hatem Zeineldin. Overview of maximum power point tracking technologies for photovoltaic power systems. In *IECON 2011-37th Annual Conference on IEEE Industrial Electronics Society*, pages 3900–3905. IEEE, 2011.

**Nomenclature**

a Coefficient temperature of $I_{sc}$

C Capacitor

D Duty cycle

$D_1$ Schottky diode

$E_g$ Band gap voltage of silicon

f(x) function

G Radiation in w/$m^2$

$G_0$ Nominal value of irradiance

I Output current of PV cell

$I_0$ Diode reverse saturation current

$I_{SC}$ Short circuit current

IC Incremental Conductance

k Boltzman constant

$L_1$ Input inductor of Cuk converter

$L_2$ Output inductor of Cuk converter

MPP Maximum Power Point

MPPT Maximum Power Point Tracking

MRFM Modified Regula Falsi Method

n Ideality factor of diode

P&O Perturb$Observe

PV Photovoltaic

q Charge of electron

$R_s$ Series resistance of PV cell

RFM Regula Falsi Method

SW Switch of Cuk converter

T Module temperature

$T_{ref}$ Reference temperature of PV cell

V Cell voltage

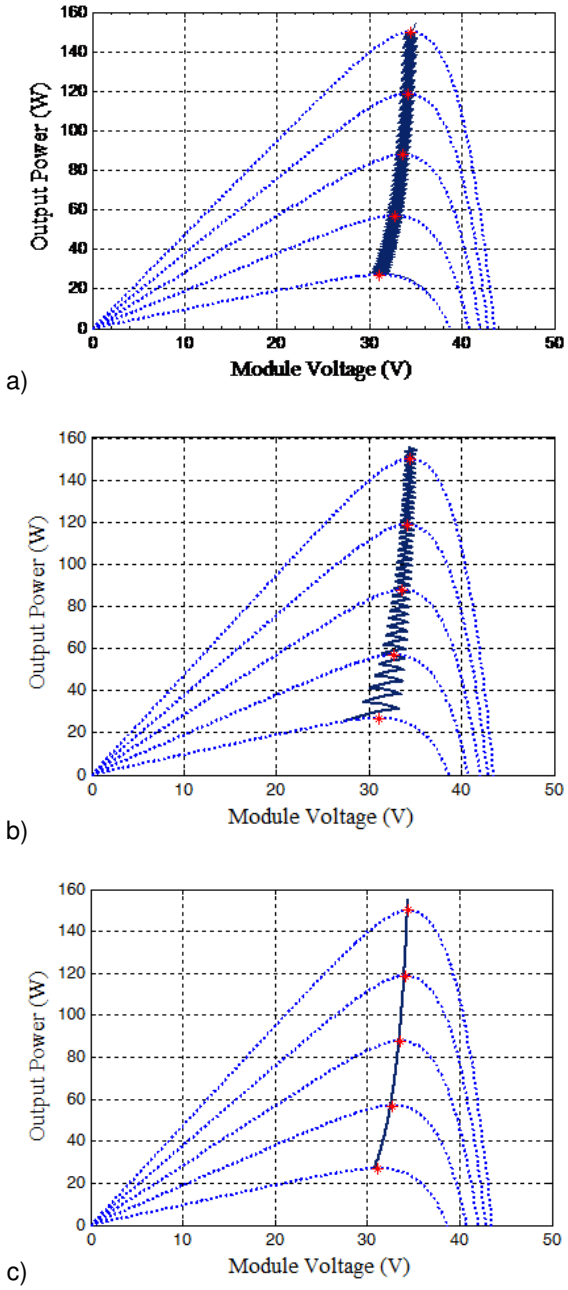


Figure 7: Graph between output powers (W) and modular voltage (V) for (a) P&O (b) IC and (c) MRFM technique

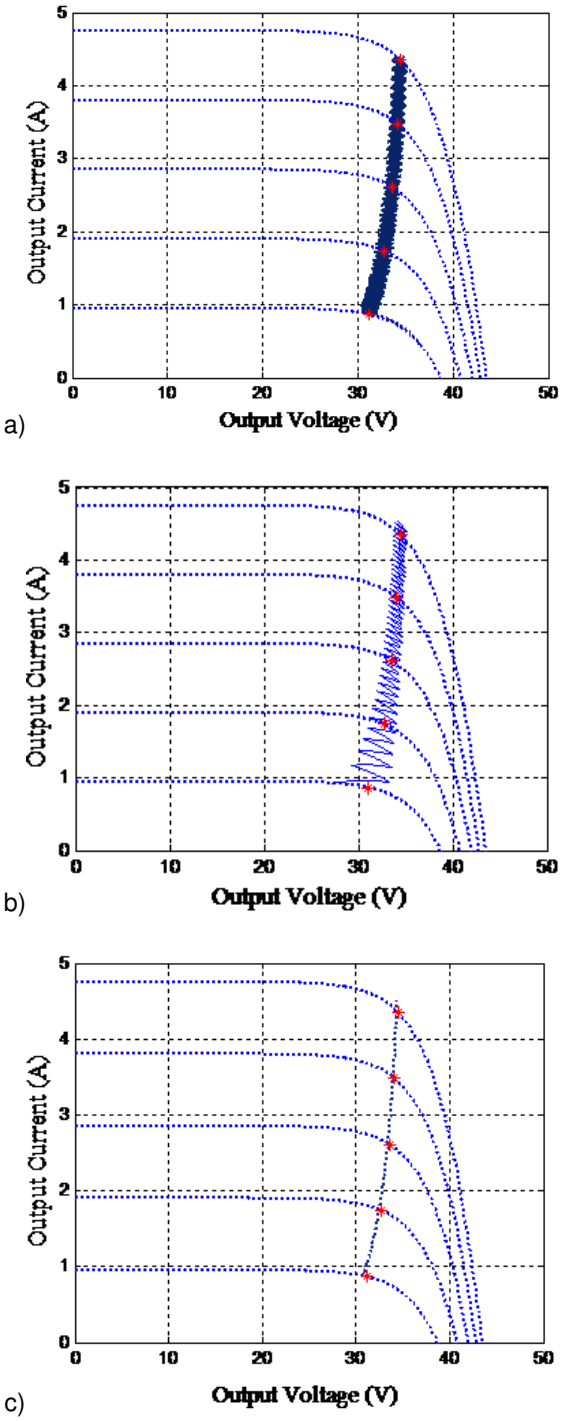


Figure 8: Graph between output current (A) and output voltage (V) for (a) P&O (b) IC and (c) MRFM technique

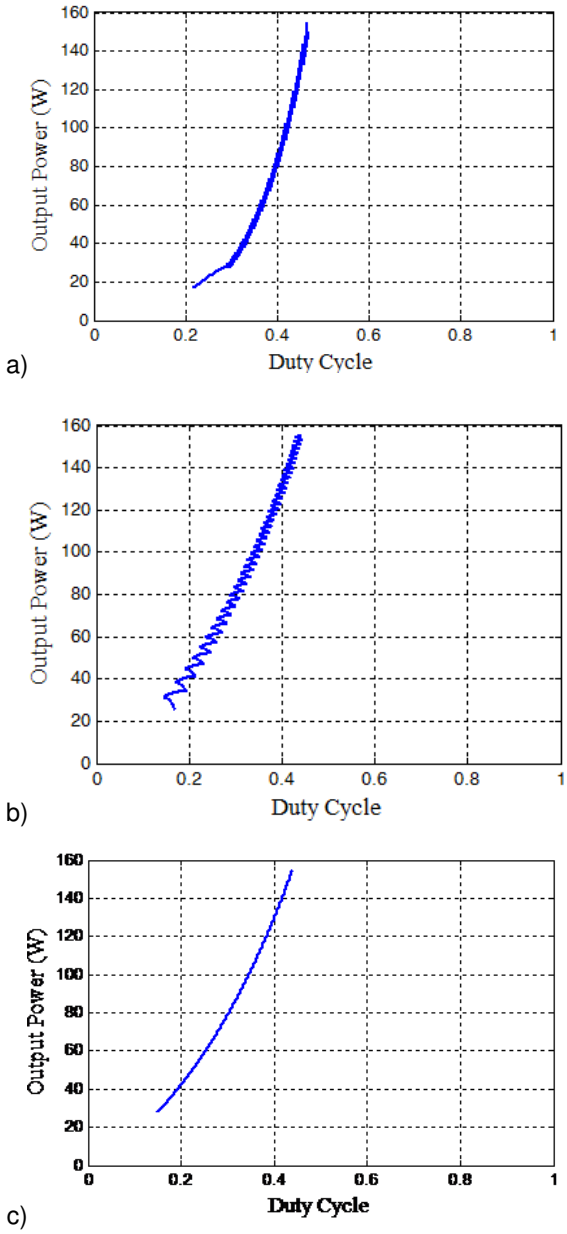


Figure 9: Graph between output power (W) and duty cycle for (a) P&O (b) IC and (c) MRFM techniques

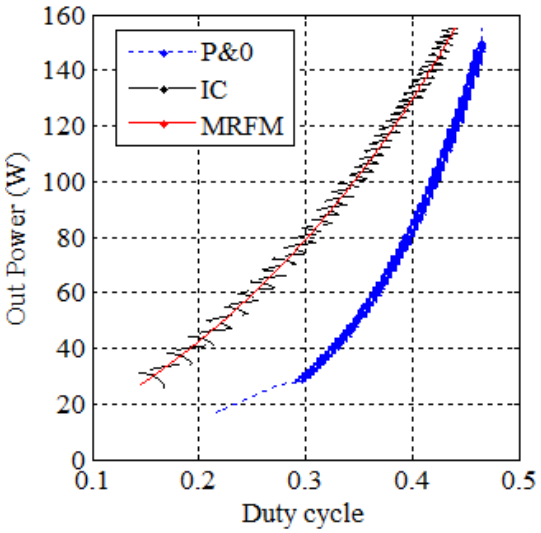


Figure 10: Comparision of the graph of the P&O, IC and MRFM techniques between output power (W) and duty cycle

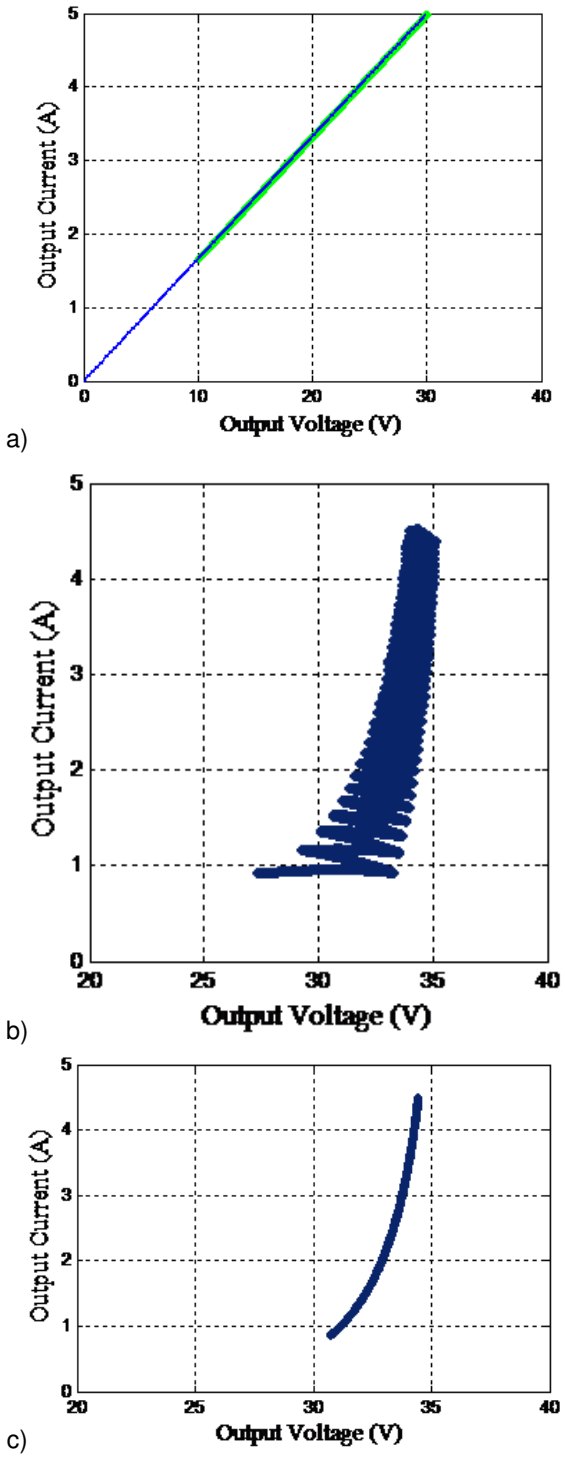


Figure 11: Graph between Cuk converter output current and voltage for (a) P&O (b) IC and (c) MRFM techniques